Selenium Speciation Assessed by X-Ray Absorption Spectroscopy of Sequentially Extracted Anaerobic Biofilms

ARTICLE *in* ENVIRONMENTAL SCIENCE AND TECHNOLOGY · NOVEMBER 2008

Impact Factor: 5.33 · DOI: 10.1021/es800811q · Source: OAI

Article

Selenium Speciation Assessed by X-Ray Absorption Spectroscopy of Sequentially Extracted Anaerobic Biofilms

Markus Lenz, Eric D. van Hullebusch, Franc#ois Farges, Sergei Nikitenko, Camelia N. Borca, Daniel Grolimund, and Piet N. L. Lens

Environ. Sci. Technol., **2008**, 42 (20), 7587-7593 • DOI: 10.1021/es800811q • Publication Date (Web): 09 September 2008

Selenium Speciation Assessed by X-Ray Absorption Spectroscopy of Sequentially Extracted Anaerobic Biofilms

MARKUS LENZ,[†,▽] ERIC D. VAN HULLEBUSCH,[†,‡] FRANÇOIS FARGES,[§] SERGEI NIKITENKO,[∥] CAMELIA N. BORCA,[⊥] DANIEL GROLIMUND,[⊥] AND PIET N. L. LENS*[,†,#]

Sub-Department of Environmental Technology, Wageningen University, 6700 EV Wageningen, The Netherlands, Laboratoire Géomatériaux et Géologie de l'Ingénieur (G2I), Université Paris-Est, EA 4119, 5 bd Descartes, 77454 Marne la Vallée Cedex 2, France, Museum National d'Histoire Naturelle de Paris, USM 201 minéralogie-Pétrologie and UMR CNRS 7160, Paris, France, Department of Geological and Environmental Sciences, Stanford University, California 94305-2115, Netherlands Organization for Scientific Research (NWO), DUBBLE at European Synchrotron Radiation Facility (ESRF), BP 220, 38043 Grenoble Cedex 9, France, Paul Scherrer Institut−Swiss Light Source, 5232 Villigen, Switzerland, UNESCO-IHE Institute for Water Education, Westvest 7, 2611 AX Delft, The Netherlands, and Institute for Ecopreneurship, University of Applied Sciences Northwestern Switzerland (FHNW), Gründenstrasse 40, 4132 Muttenz, Switzerland

Received March 21, 2008. Revised manuscript received May 24, 2008. Accepted May 26, 2008.

Wet chemical methods such as sequential extraction procedures are commonly used to assess selenium fractionation in anoxic environments, allowing an estimation of the mobility and bioavailability of selenium. However, the interpretation can be biased by unselective extraction of targeted species and artifacts introduced during the extraction. Here, the selectivity of the single extraction steps to gain reliable selenium speciation information are scrutinized for the first time by direct, nondestructive X-ray absorption near edge structure (XANES) spectroscopy at the selenium K-edge. The sequential extraction procedures seriously overestimated the elemental selenium fraction, as major parts (58%) of the total selenium were present as metal selenides and organic selenium compounds, although extracted in the elemental fraction. Spectral fitting of the XANES spectra by the least-squares linear combinations utilizing a large set of model compounds, including previously neglected Se(−I) selenides, showed a novel degree of complexity in the speciation of selenium treating anaerobic biofilms, with up to 4 modeled selenium species contributing to the speciation, i.e., different elemental, organic, and metal-bound selenium species. Furthermore, a short exposure (10 min) to ambient air during the sequential extraction procedure induced the oxidation of organic selenium compounds, revealing the fragility of selenium speciation in anaerobic biofilms.

1. Introduction

Selenium is characterized by its dual character of being both essential and toxic to living organisms (*1*). It is present in the environment in at least five oxidation states (−II, −I, 0, IV, VI) in a variety of organic and inorganic compounds (*2*). The environmental fate and the toxicity of selenium strongly depends on its chemical speciation (*3*), thus a determination of the total selenium content is insufficient to assess the impact of selenium contamination. Water soluble, oxidized forms (selenite and selenate) cause severe damage to wildlife (*4*) and need to be removed from aqueous (waste)streams, consequently. Microorganisms can mediate a reduction of these oxyanions to less toxic, insoluble elemental selenium (*5*). Nevertheless, different intermediate or side products are biogenically formed, including, for example, highly toxic H_2Se (*6*) or bioavailable organic forms like selenoamino-acids (*7*).

To estimate risks posed by selenium contamination, sequential extraction procedures (SEPs) operationally define fractions of selenium by applying different extractants and extraction conditions (*8–12*). As SEPs do not require sophisticated analytical equipment and allow multiple sample processing, they can be used on a routine basis. Although applied to anoxic environments like sediments (*9, 10*) or deep soil layers (*13, 14*), the alteration of selenium speciation by oxidation through ambient air during extraction has thus far not been given attention (*15, 16*). In this context, the fractionation can be biased by both oxidation of the matrix, e.g., oxidation of sulfides (*17*), or by changes in selenium speciation (*14*). If the speciation is not preserved or the SEPs are not selective for the targeted species, bioavailable fractions can be seriously misinterpreted.

This paper investigates the speciation changes during short exposure to ambient air as they occur, e.g., during field sampling or sample preparation. The applicability of SEPs is tested on a particular type of selenate reducing biofilms, so-called anaerobic granular sludge, sampled from upflow anaerobic sludge bed (UASB) reactors treating selenate contaminated synthetic wastewater under methanogenic conditions (*18*). These anaerobic granules are 2−4 mm in diameter and consist of biomass closely associated with an inorganic, metal sulfide rich matrix (*19, 20*).

Solid-phase speciation and changes induced by ambient air were assessed by X-ray absorption near edge structure (XANES) spectroscopy. Linear combinations with a variety of natural and synthetic reference model compounds were used to assess the local structural environment. Special care was given to assess the presence of Se (−I), a valence state that has often been neglected in past XANES studies. Furthermore, selenium model compounds that have previously not been included in SEP studies (aqueous selenide and selenocysteine) were added to the anaerobic biofilm and the possible influence of oxidation by ambient air on selenium fractionation was investigated.

2. Experimental Section

2.1. Source of Biomass. Anaerobic granular sludge from a full scale UASB reactor treating paper mill wastewater

* Corresponding author e-mail: Piet.Lens@wur.nl.
† Wageningen University.
‡ Université Paris-Est.
§ Museum National d'Histoire Naturelle de Paris, USM 201 minéralogie-Pétrologie and UMR CNRS 7160, and Stanford University.
∥ Netherlands Organization for Scientific Research (NWO), DUBBLE at European Synchrotron Radiation Facility (ESRF).
⊥ Paul Scherrer Institut−Swiss Light Source.
UNESCO-IHE Institute for Water Education.
▽ University of Applied Sciences Northwestern Switzerland (FHNW).

10.1021/es800811q CCC: $40.75
Published on Web 09/09/2008

TABLE 1. Chemical Composition of the Bioreactor Influent and the Investigated Biofilm

influent composition (mmol per L)		biofilm elemental composition (mg per kg dry weight)	
NH_4Cl	5.6	Ca	48113 ± 3648
NaCl	5.1	Co	105 ± 4
$CaCl_2 \cdot 2H_2O$	0.7	Cu	150 ± 1
$MgCl_2 \cdot 6H_2O$	0.5	Fe	11140 ± 808
KH_2PO_4	16.8	K	7930 ± 208
$Na_2HPO_4 \cdot 2H_2O$	23.1	Mg	1861 ± 58
		Mn	168 ± 5
influent composition (μmol per L)		Na	7969 ± 259
		Ni	149 ± 3
$FeCl_2$	7.5	Pb	37 ± 3
H_3BO_4	1	S	11822 ± 684
$ZnCl_2$	0.5	Se	414 ± 25
$CuCl_2$	0.1	Zn	331 ± 9
$MnCl_2$	0.5		
$CoCl_2$	0.5		
$NiCl_2$	0.1		
Na_2WO_4	0.1		
Na_2MoO_4	0.1		

(Industriewater Eerbeek B.V., Eerbeek, The Netherlands) was utilized for the standard extraction experiments and as inoculum for a laboratory-scale bioreactor. Under methanogenic conditions (pH 7.0; 30 °C) selenate and lactate were fed at 40 μmol selenate (L of reactor volume)$^{-1}$ d^{-1} and 1.9 g of lactate (L of reactor volume)$^{-1}$ d^{-1} (21 mmol (L of reactor volume)$^{-1}$ d^{-1}), respectively (*21*). Table 1 gives the reactor influent composition. Biomass of the laboratory-scale reactor was harvested after 60 days of operation and SEPs were applied to this sludge. The Biofilm elemental composition (Table 1) was determined by a Varian Vista-MPX CCD (Middleburg, The Netherlands) inductively coupled plasma optical emission spectroscopy (ICP-OES) (*22*).

2.2. Standards Extraction. Granular sludge was autoclaved for 20 min at 121 °C, either anoxically in glass serum bottles sealed with a butyl rubber stopper and flushed with N_2 or in cotton plugged aerobic glass serum bottles. Selenocysteine (ultrapure quality; Sigma-Aldrich, Zwijndrecht, Netherlands) was added to the autoclaved sludge (0.15 g wet weight) in solid form using an Ultrafine balance (AT21, Mettler Toledo, Tiel, Netherlands), whereas sodium selenide (ultrapure quality; Alfa Aesar, Karlsruhe, Germany) was dissolved in an anoxic stock solution (phosphate buffer, 40 mM, pH 7.0 ± 0.1) and added by pipetting.

2.3. Sequential Extractions. SEPs for selenium fractionation were done as previously described (*9*), but using a 10 times higher extractant to solid ratio, due to incomplete selenium recoveries observed in pre-experiments. Prior to the extraction, the samples were homogenized using a glass stick. Briefly, fraction 1 targeted soluble/exchangeable selenium (extraction with 0.25 M KCl), fraction 2 the adsorbed selenium (extraction with 0.1 M K_2HPO_4), fraction 3 elemental selenium (extraction with 0.25 M Na_2SO_3, sonication at 20 kHz for 2 min, then ultrasonic bath for 4 h), and fraction 4 so-called "organically associated selenium" (extraction with 5% NaOCl).

The SEPs were carried out either under a N_2 atmosphere in a glovebox or aerobically on the laboratory bench, exposing the samples for 10 min to ambient air prior to continuation with each extraction step. In the case of the anoxic extraction, centrifugation was conducted in airtight high purity polypropylene copolymer (PPCO) vials (Nalgene, Neerijse, Belgium).

Subsequent to each extraction step, one batch of the respective samples was placed in a custom-made sample holder of polytetrafluoroethylene using the glovebox. Samples were sealed from ambient air by kapton tape. The sample holders were stored (4 °C) under N_2 in a wide mouth bottle until the XANES measurements. The residues of the first, second, and third extraction step are referred to as R1, R2, and R3, whereas residues of extraction conducted under ambient air are referred to as "O_2" and anoxic extractions as "N_2". The selenium content in the samples after the fourth extraction step was low, thus XANES spectra for R4 could not be recorded during the beam time available.

2.4. Selenium Solid-State Speciation. Selenium K-edge (12.66 keV) XANES experiments were performed at the DUBBLE beamline (BM26, ESRF,Grenoble France) and at the microXAS beamline (X05, SLS, Villingen, Switzerland). The first beamline was used to obtain systematic "bulk" XANES information, whereas the second beamline was used to collect μ-XANES spectra on selected areas of the reference compounds. At the ESRF, a focused beam (~0.2 × 3 mm) with a 9-element solid-state Ge detector was used. At the SLS, a microfocused beam (~3 × 3 μm^2) with a 32-elements solid-state Ge-detector was utilized. At both beamlines, Si(111) double-crystal monochromators were applied, ensuring a comparable energy resolution of about 2.5 eV at 13 KeV. The energy calibration for both monochromators was achieved using a thin film of gray, trigonal selenium placed between two ionization chambers (transmission mode) during all measurements, using the main crest edge at 12662.5 eV. All biofilm samples were collected in fluorescence mode, placed at an angle of 45° relative to the incoming X-ray beam, whereas model compounds were simultaneously measured in both transmission and fluorescence mode. Fluorescence of the reference compounds was measured an angle of 90° relative to the incoming X-ray beam in order to minimize self-absorption effects. No photoreduction due to the X-ray beam was observed during the measurements.

An overview of different natural and synthetic Se model compounds (all in solid state and powdered) used in this study is given in Table 2. Model mineral compounds were verified using a Gandolfi-type micro-X-ray diffraction (μ-XRD) built at the Museum National d'Histoire Naturelle (MNHN), Paris (*23*).

2.5. XAFS Data Reduction and Calculations. XANES spectra were normalized using the X-ray absorption fine structure (XAFS) software package (*24*) using standard procedures (*25*). Least square linear combination XANES fittings were done using MS Excel SOLVER (range between 12 635 and 12 720 eV). Principal component analysis (PCA) using the normalized spectra of all residues was done with the XANES dactyloscope software (*26*).

3. Results

3.1. XANES Calibration for the Oxidation State in Selenium Compounds. Sodium selenate and sodium selenite showed the highest energies regarding the position of the first inflection point and main edge crest (Figure 1A, Table 2). For the gray-trigonal and the α-red polymorph of elemental selenium, a difference of +0.4 eV between the main edge crest and +1.6 eV between the first inflection point was observed, respectively. Isometric−diploidal Se(−I) compounds penroseite [(Ni, Co, Cu)Se_2] and krutaite ($CuSe_2$) display virtually identical main edge crests and first inflection point positions in their XANES spectra and were thus clearly different from orthorhombic-dipyramidal Se (−I) ferroselite ($FeSe_2$) showing a shift of +0.7 eV in main edge crest and approximately +1.0 eV in the position of the first inflection point (Figure 1B, Table 2).

Cubic Se(−II) compounds were shifted up to + 4.6 eV in the main edge crest (berzelianite, Cu_2Se, versus achavalite, FeSe, and klockmannite, CuSe) and up to +3.1 eV (berzelianite versus achavalite) in the first inflection point compared to dihexagonal−dipyramidal forms (Figure 1B, Table 2). Within

TABLE 2. Selenium Model Compounds and Residues of the Sequential Extractions Investigated in This Study

specimen	chemical formula	origin	formal oxidation state	cryst syst	space group	main edge crest (eV)	first inflection point (eV)
red α-monoclinic Se (0)	Se	synthetic	0	monoclinic	*P2/n*	12662.1	12659.5
penroseite	$(Ni,Co,Cu)Se_2$	Bolivia	−I	isometric−diploidal	*Pa3*	12662.1	12659.9
krutaite	$CuSe_2$	Bolivia	−I	isometric−diploidal	*Pa3*	12662.1	12659.8
achavalite	FeSe	synthetic	−II	dihexagonal dipyramidal	*P6/mmc*	12662.3	12659.9
klockmannite	CuSe	synthetic	−II	dihexagonal dipyramidal	*P6/mmc*	12662.3	12660.0
selenocysteine	$C_3H_7NO_2Se$	synthetic	−II			12663.4	12660.7
ferroselite	$FeSe_2$	Utah (USA)	−I	orthorhombic−dipyramidal	*Pnnm*	12662.8	12660.9
grey trigonal Se (0)	Se	New Mexico (USA)	0	trigonal	*P321*	12662.5	12661.1
sodium selenide	Na_2Se	synthetic	−II	cubic	*Fm3m*	12665.8	12661.1
stilleite	ZnSe	synthetic	−II	cubic	*F43m*	12665.7	12662.9
berzelianite	Cu_2Se	Czech Republic	−II	cubic	*F43m*	12666.6	12663.0
sodium Selenite	Na_2SeO_3	synthetic	+IV	monoclinic	*P2/c*	12667.2	12664.7
sodium Selenate	Na_2SeO_4	synthetic	+VI	orthorhombic	*Fddd*	12670.2	12667.5

specimen	extraction condition	residue	main edge crest [eV]	first inflection point [eV]
$R1N_2$	N_2	1st	12662.8	12660.6
$R2N_2$	N_2	2nd	12662.9	12660.8
$R3N_2$	N_2	3rd	12662.6	12660.0
$R1O_2$	O_2	1st	12662.3	12660.1
$R2O_2$	O_2	2nd	12662.2	12659.9
$R3O_3$	O_2	3rd	12662.8	12660.9

the cubic Se(−II) compounds, a shift was observed in the first inflection point of the XANES spectra considering different mineral space groups, i.e., *F*43*m* and *Fm*3*m*. Minerals with *F*43*m* (stilleite, ZnSe, and berzelianite) were clearly shifted in comparison to sodium selenide with F m3m space group (+1.8 eV) (Table 2). Selenocysteine was clearly different from all other Se(−II) compounds regarding both features.

3.2. Effect of Ambient Air on Fractionation by Sequential Extraction. The standards extraction demonstrated that selenocysteine was extracted mainly in the soluble/exchangeable fraction, while minor parts adsorbed to the sludge, independent from the presence or absence of oxygen (Table 3). Selenide was found to higher amounts in the elemental fraction during the aerobic extraction (88.6% versus 72.1%) and more selenium was yielded in the organically associated and residual fraction when treated anoxically (Table 3). Only minor differences were noted in the soluble/exchangeable and adsorbed fractions. Red precipitates (probably red elemental selenium) were noted upon addition of the selenide solution in both extractions, although the anoxic aqueous stock solution was stable.

The SEPs conducted with selenium containing bioreactor sludge yielded most selenium in the elemental fraction (fraction III), while minor amounts (≤1.5% in the presence of N_2; ≤ 2.5% in the presence of air) were found in the other fractions (Table 3). Extraction in the presence of air resulted in a larger elemental fraction, but total selenium recoveries were higher compared to the anoxic extraction.

The selenium K-edge XANES spectra of the residues obtained after the first (R1) and second (R2) sequential extraction step displayed a shifted main crest edge (≤+0.7 eV) and inflection point (≤+0.9 eV) when the SEP was conducted anoxically (RxN_2) in comparison to extraction under ambient air (RxO_2) (Figure 1C, Table 2). A shift (−0.9 eV) in the first inflection point position was determined in the third residue ($R3O_2$ versus $R3N_2$).

Linear combinations suggested that the first two residuals extracted anoxically ($R1N_2$ and $R2N_2$) were mainly composed of compounds related to trigonal Se(0) and cubic Se(−II) selenides (stilleite) (Table 3) 2A). Minor contributions were due to organic selenium (related to selenocysteine) and selenite in R1 and to selenite/selenate in R2, respectively. Trigonal Se(0) and cubic Se(−II) (sodium selenide)-like compounds were mainly contributing to the modeled $R3N_2$ spectrum. In contrast, a dihexagonal-dipyamidal (klockmannite) type mineral and selenate contributed to the selenium speciation in $R1O_2$ and $R2O_2$. A marginal contribution (3%) of selenate to $R3O_2$ is reported but not considered further.

4. Discussion

4.1. Determination of Selenium Valence and the Coordination Environment via XANES. This study shows that the main edge crest ("white line") position and the first inflection point should be used in combination to assess the selenium speciation by XANES (valence and local geometry) in a more robust way, as different valences can show the same main edge crest or first inflection point (Table 2, Figure 1A) due to interferences from the signals arising from the local geometry interactions. However, this requires a highly precise determination of the position of these features that can be shifted by 0.2 eV only (e.g., achavalite vs penroseite, Table 2). In contrast to sulfur K-edge XANES (*27*), a main edge crest or the first inflection point shifted to lower energies does not imply a more reduced oxidation state (e.g., red α-Se(0) showed the lowest main edge crest and inflection point, Table 2). Nevertheless, selenate (+VI) and selenite (+IV), members of the highest oxidation states, showed these

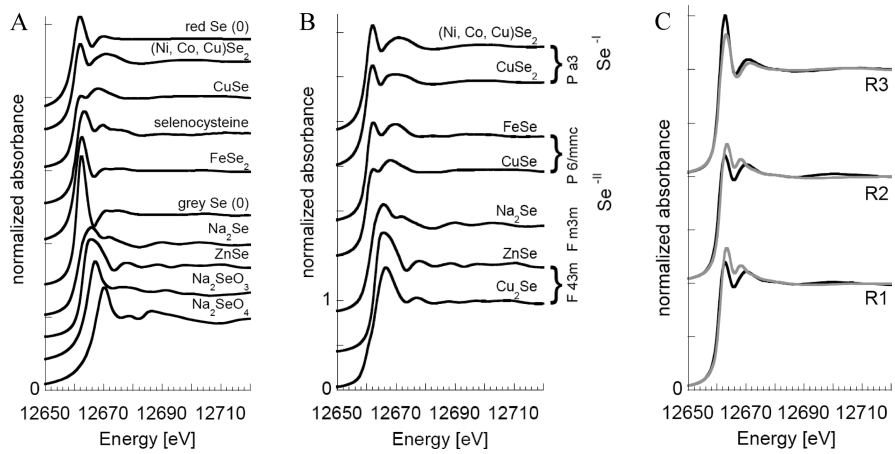

FIGURE 1. Normalized Se K-edge XANES spectra for model compounds (A and B) and residues of the sequential extractions (C) conducted anoxically (gray line) and in the presence of ambient air (black line).

TABLE 3. Selenium Fractionation by Sequential Extraction (Bioreactor Samples and Standards Extractions) (Top) and Selenium Speciation Modeled by Linear Combination of XANES Spectra (Bottom)

sample	extraction condition	soluble/ exchangeable (fraction 1)	adsorbed (fraction 2)	elemental (fraction 3)	organically associated (fraction 4)	residual	Σ
bioreactor sludge	O_2	2.0 ± 0.3	2.5 ± 0.1	109.2 ± 1.9	0.2 ± 0.0	0.5 ± 0.3	114.4
	N_2	0.8 ± 0.1	1.5 ± 0.1	86.8 ± 4.8	0.4 ± 0.1	0.7 ± 0.3	90.2
selenocysteine	O_2	88.1 ± 2.7	8.5 ± 1.9	1.0 ± 0.2	0.1 ± 0.0	0.1 ± 0.0	97.9
	N_2	87.8 ± 1.6	7.8 ± 0.1	2.3 ± 0.3	0.3 ± 0.0	0.1 ± 0.0	98.2
HSe^-	O_2	2.7 ± 0.2	0.5 ± 0.1	88.6 ± 2.1	7.3 ± 0.2	1.4 ± 0.6	100.5
	N_2	2.2 ± 0.3	0.2 ± 0.0	72.1 ± 2.6	19.9 ± 1.3	7.0 ± 1.1	101.4

$R1O_2$	41% gray Se (0)	16% Na_2SeO_4	(14% CuSe)	(11% Cu_2Se)
$R1N_2$	45% gray Se (0)	41% ZnSe	(7% Selenocysteine)	(5% selenite)
$R2O_2$	40% gray Se (0)	27% CuSe	(15% Na_2SeO_4)	(10% Na_2Se)
$R2N_2$	47% gray Se (0)	44% ZnSe	(5% selenite)	(3% Na_2SeO_4)
$R3O_2$	70% gray Se (0)	14% ZnSe	(8% Na_2Se)	(4% FeSe)
$R3N_2$	54% gray Se (0)	26% Na_2Se	(10% ZnSe)	(10% Na_2SeO_4)

features at higher energies, in agreement with a number of previous studies (*28–30*).

In the past, numerous studies have exclusively utilized the main edge crest ("white line") position (*2, 29, 31, 3*) or the first inflection point (*30, 34, 35*) to determine the selenium oxidation state, which was already a large improvement toward obtaining accurate values for valences of selenium. However, the present set of model compounds shows that this protocol requires major adjustments. Furthermore, the use of the main edge crest relative intensity to determine oxidation states of selenium at the Se K-edge (*36*) works well on iron selenides, but not on copper selenides (Figure 1B). Therefore, this method must be discarded. Within the set of model compounds investigated in this study (including rarely described Se(−I) selenides used for the first time) and using both features simultaneously, it was possible to differentiate between coordination geometries of selenium compounds of the same valence, e.g., sodium selenide versus stilleite/berzelianite and versus achavalite/klockmannite (Table 2, Figure 1B).

4.2. Selenium Speciation in Methanogenic Granular Sludge. An accurate description of selenium speciation in anaerobic biological samples, e.g. methanogenic granules, can be achieved by the investigated set of model compounds (Table 2) using linear combinations, demonstrated by the accurate best fits shown in Figure 2A and B. Although the number of reference compounds used to model the experimental XANES spectra was limited as much as possible, considerably better fits were achieved using 4 model compounds, demonstrating the complexity of selenium speciation in selenate treating UASB granules. PCA of the selenium K-edge XANES was limited to the theoretically four most abundant species, but two most abundant species are significantly influencing the speciation of selenium, only. Accordingly, two components are actually dominant in most models: trigonal Se(0) is dominant in all residues, stilleite or

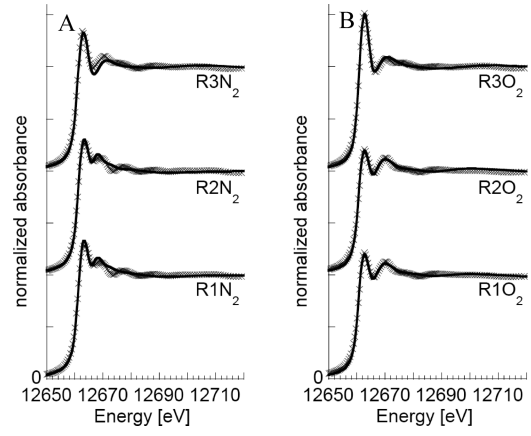

FIGURE 2. Normalized Se K-edge XANES spectra for sequential extraction residues R1 to R3 (solid lines) and best fit by linear combination to model compounds (×) after extraction performed anoxically (A) and under ambient air (B). Contributions of model compounds (Table 2) to the best fit results are given in at %. Misfits are related to unidentified selenium species.

sodium selenide are relevant in the anoxic extractions, while klockmannite/stilleite or selenate are determining selenium speciation in the aerobic extraction (Table 3). Thus, this confirms that two components are significantly determining the selenium speciation in the investigated samples.

It can be assumed that the speciation of the bioreactor sludge during treatment of selenium containing wastewater is close to the modeled speciation in $R1N_2$ due to the fact that only minor amounts (0.8%) of soluble/exchangeable selenium were extracted (Table 3) and that the extractant ions (0.25 M KCl) are constituents of the bioreactor feed (Table 1). The XANES model demonstrated that most selenium (86%) was present in Se(0) and Se(−II) cubic form, thus confirming the ability of methanogenic UASB reactors to immobilize bioavailable (water soluble) selenium oxyanions to insoluble mineral phases (*21*). The fact that so far no metal selenide was detected by XRD methods in these sludges (*22, 37*) can be explained by nanocrystallized forms (*38*). Indeed, when operated continuously in UASB reactors under methanogenic conditions, anaerobic granular sludge converts selenate to selenium containing particles of <200 nm particle size, colloidally dispersed in the effluent (*21*). Although lactate was fed in large molar excess compared to selenate, theoretically favoring the reduction to selenides (*39*), elemental selenium was the main reduction product (Table 3). This can be explained by a conversion of major parts of the electron donor (lactate) to methane and residual volatile fatty acids, reducing the amount of electron donor available for selenate reduction.

The minor contribution of selenocysteine observed here can represent a precursor to selenium alkylation (*40*), as the sludges form dimethylselenide and dimethyldiselenide from endogenous selenium sources (*21*). In a previous study (*21*), selenium speciation in anaerobic sludge granules was found to be mainly determined by elemental selenium. The higher contribution of elemental selenium to the modeled selenium speciation observed previously can be explained by the longer reactor operation upon sludge sampling, if more selenium is fixed in the biomass as elemental selenium in comparison to metal selenides upon prolonged reactor operation.

In general, experimental XANES spectra obtained in methanogenic granules are fairly well represented by the combination of model compounds used here (Figure 2). Under high sulfur conditions, e.g., in sulfate reducing biofilms (*21*), however, the interpretation of the XANES spectra might be complicated by the fact that selenium can be replaced by sulfur and precipitated selenides might comprise mixtures in different selenium/sulfur ratio, e.g., as mixed FeS/Se (*41*), and thus further reference compounds need to be studied for these cases.

4.3. Influence of Ambient Air on Selenium Speciation/Fractionation. This study shows that a short exposure (10 min) to ambient air, likely to occur during field sampling of, for example, contaminated sediments or anaerobic bioremediation systems, can induce a change in selenium speciation (Table 3, Figure 1C) and consequently fractionation (Table 3) in anaerobic biofilms.

The fitting of the XANES spectra showed the presence of a highly oxidized (selenate like) species in $R1O_2$ and $R2O_2$, which can be explained by the oxidation of stilleite on the one hand and complete oxidation of organic (selenocysteine like) species (*42, 43*) to selenate (Table 3, $R1N_2$ versus $R1O_2$) on the one hand. However, this oxidation is not reflected in different selenium yields in the first fractions of the SEP investigated, as both selenate (*9*) and selenocysteine are coextracted in this fraction (Table 3). For the disposal of bioreactor excess sludge under aerobic conditions, selenate formation is particularly problematic as it adsorbs only badly to the sludge matrix (*37*) and might thus leach out.

In $R1O_2$ and $R2O_2$, a dihexagonal-dipyramidal Se(−II) selenide of klockmannite type (space group *P*6/*mmc*, Table 2) was found in the best fitted linear combinations, in contrast to a F 43m cubic Se(−II) selenide (here: stilleite) in $R1N_2$ and $R2N_2$ (Table 3). Due to the contribution of several species to the reconstructed XANES spectra and to the possible nanocrystallized character hindering exact identification by XRD (*38*), a precise mechanism for the mineral transition observed here cannot be assigned. Hypothetically, parallels to sulfur mineral chemistry might be drawn, where a transformation of chalcocite (Cu_2S) to covellite (CuS) by oxygen in sulfate solutions has been demonstrated (*44*). To the best of our knowledge, the direct evidence of the berzelianite (Cu_2Se, *F*43*m*) oxidation to klockmannite (CuSe, *P*6/*mmc*) by ambient air has not been described in the literature. A time-resolved μ-XRF study could shed light on this oxidation mechanism. Yet, alternative selenides with the same space group (P 6/mmc) (e.g., freboldite (CoSe, p*K*s = 31.2) or sederholmite (NiSe, p*K*s = 32.7) (*45*)) should also yield similar XANES fittings, and both cobalt and nickel are present in the bioreactor feed and in the harvested sludge (Table 1). Replacing copper by cobalt or nickel (at a constant space group) should not affect the XANES models presented here.

The reconstructed XANES spectra suggest that the change in speciation of $R3O_2$ in comparison to $R3N_2$ (Figure 1C) was attributed to the oxidation of a cubic (sodium selenide) Se(−II) type to elemental selenium (Table 3). However, the presence of sodium selenide as such is unlikely, as it is water soluble. It was furthermore demonstrated that aqueous selenide is highly labile even under strict anoxic conditions and instantly oxidized to elemental selenium, as a red colored precipitate formed upon addition to the sludge and the SEP yielded most selenium in the elemental fraction (Table 3), although insoluble selenides might also form, suggested by the so-called "organically associated" fraction. Persistence of aqueous selenide formed by microbial processes (*6, 39, 41*) is thus unlikely in metal rich environments, e.g., anaerobic granular sludge or contaminated sediments, providing a sink for highly toxic aqueous selenide. Alternatively, an insoluble cubic Se(−II) type with a *Fm*3*m* space group might rather explain the modeled selenium speciation in $R3N_2$.

4.4. Extraction Selectivity of the SEP. This study shows that the SEP achieves selectivity for selenocysteine, as mainly found in the soluble/exchangeable fraction (Table 3) in the standards extraction experiments and furthermore only contributing to the modeled speciation of $R1N_2$, but not $R2N_2$. Selenate however, targeted in fraction 1 (*9*) contributed to the speciation of $R1O_2$ (Table 3) and is thus insufficiently extracted. The selectivity for elemental selenium targeted in fraction 3 is poor, as the decomposition of the XANES spectra suggested a high contribution of Se(0) like species to $R3O_2$ and $R3N_2$. Furthermore, the contribution of stilleite decreased between $R2N_2$ and $R3N_2$ (Table 3), demonstrating that the dissolution of these minerals leads to an overestimation of the elemental fraction, as observed by the high amounts of selenium yielded in the elemental fraction (Table 3). This implies a serious misinterpretation when evaluating detoxification from selenate by formation of elemental selenium in bioremediation applications.

In summary, this study shows that the applied SEP, although validated for several selenium species (*9*), gives an inaccurate description of the actual selenium speciation in complex matrixes including anaerobic granular sludge. Such a selectivity lack using sequential extraction procedures has previously been demonstrated by a XAS study for reduced sulfur species (*46*). While sulfur fractionation determined by sequential extraction procedures can be verified in conjunction with alternative wet chemical methods, i.e., acid volatile sulfur (*47*), such routine methods have not yet been developed for selenium fractionation. Thus, the precise description of the selenium solid phase speciation relies on nondestructive,

direct, species specific analytical methods, such as XAFS using careful speciation modeling with a sufficiently large number of selenium model compounds as the coordination chemistry of selenium under reducing conditions needs more thorough investigations.

Acknowledgments

This work was supported by the European Union within the Marie Curie Excellence TEAM Grant "Novel biogeological engineering processes for heavy metal removal and recovery" (MEXT-CT-2003-509567). The work was further supported by The Netherlands Organization for Scientific Research (Nederlandse Organisatie voor Wetenschappelijk Onderzoek, NWO) and European Economic Community, which financed trips to ESRF and SLS. We thank the staff at DUBBLE (ESRF, Grenoble, France) and SLS (Villigen, Switzerland) for providing access to their beamlines and for their help in data collection.

Literature Cited

(1) Hamilton, S. J. Review of selenium toxicity in the aquatic food chain. *Sci. Total Environ.* **2004**, *326*, 1–31.

(2) Naveau, A.; Monteil-Rivera, F.; Guillon, E.; Dumonceau, J. Interactions of aqueous selenium (−II) and (IV) with metallic sulfide surfaces. *Environ. Sci. Technol.* **2007**, *41*, 5376–5382.

(3) Yu, R.; Coffman, J. P.; Van Fleet Stalder, V.; Chasteen, T. G. Toxicity of oxyanions of selenium and of a proposed bioremediation intermediate, dimethyl selenone. *Environ. Toxicol. Chem.* **1997**, *16*, 140–145.

(4) Wu, L. Review of 15 years of research on ecotoxicology and remediation of land contaminated by agricultural drainage sediment rich in selenium. *Ecotoxicol. Environ. Saf.* **2004**, *57*, 257–269.

(5) Oremland, R. S.; Hollibaugh, J. T.; Maest, A. S.; Presser, T. S.; Miller, L. G.; Culbertson, C. W. Selenate reduction to elemental selenium by anaerobic bacteria in sediments and culture: biogeochemical significance of a novel, sulfate-independent respiration. *Appl. Environ. Microbiol.* **1989**, *55*, 2333–2343.

(6) Zehr, J. P.; Oremland, R. S. Reduction of selenate to selenide by sulfate-respiring bacteria: Experiments with cell suspensions and estuarine sediments. *Appl. Environ. Microbiol.* **1987**, *53*, 1365–1369.

(7) Turner, R. J.; Weiner, J. H.; Taylor, D. E. Selenium metabolism in *Escherichia coli*. *Biometals* **1998**, *11*, 223–227.

(8) Profumo, A.; Spini, G.; Cucca, L.; Mannucci, B. Sequential extraction procedure for speciation of inorganic selenium in emissions and working areas. *Talanta* **2001**, *55*, 155–161.

(9) Wright, M. T.; Parker, D. R.; Amrhein, C. Critical evaluation of the ability of sequential extraction procedures to quantify discrete forms of selenium in sediments and soils. *Environ. Sci. Technol.* **2003**, *37*, 4709–4716.

(10) Martens, D. A.; Suarez, D. L. Selenium speciation of soil/sediment determined with sequential extractions and hydride generation atomic absorption spectrophotometry. *Environ. Sci. Technol.* **1997**, *31*, 133–139.

(11) Tokunagaz, T. K.; Lipton, D. S.; Benson, S. M.; Yee, A. W.; Oldfather, J. M.; Duckart, E. C.; Johannis, P. W.; Halvorsen, K. E. Soil selenium fractionation, depth profiles and time trends in a vegetated site at Kesterson Reservoir. *Water Air. Soil Pollut.* **1991**, *57* (58), 31–41.

(12) Munier-Lamy, C.; Deneux-Mustin, S.; Mustin, C.; Merlet, D.; Berthelin, J.; Leyval, C. Selenium bioavailability and uptake as affected by four different plants in a loamy clay soil with particular attention to mycorrhizae inoculated ryegrass. *J. Environ. Radioact.* **2007**, *97*, 148–158.

(13) Wang, M. C.; Chen, H. M. Forms and distribution of selenium at different depths and among particle size fractions of three Taiwan soils. *Chemosphere* **2003**, *52*, 585–593.

(14) Kulp, T. R.; Pratt, L. M. Speciation and weathering of selenium in upper cretaceous chalk and shale from South Dakota and Wyoming, USA. *Geochim. Cosmochim. Acta* **2004**, *68*, 3687–3701.

(15) Olivas, R. M.; Donard, O. F. X.; Camara, C.; Quevauviller, P. Analytical techniques applied to the speciation of selenium in environmental matrices. *Anal. Chim. Acta* **1994**, *286*, 357–370.

(16) Uden, P. C.; Boakye, H. T.; Kahakachchi, C.; Tyson, J. F. Selective detection and identification of Se containing compounds - review and recent developments. *J. Chromatogr., A* **2004**, *1050*, 85–93.

(17) Lasorsa, B.; Casas, A. A comparison of sample handling and analytical methods for determination of acid volatile sulfides in sediment. *Mar. Chem.* **1996**, *52*, 211–220.

(18) Lenz, M.; Smit, M.; Binder, P.; van Aelst, A. C.; Lens, P. N. L. Biological alkylation and colloid formation of selenium in methanogenic UASB reactors. *J. Environ. Qual.* **2008**, *37*(5), in print.

(19) Hullebusch, E. D. v.; Utomo, S.; Zandvoort, M. H.; L.; Lens, P. N. Comparison of three sequential extraction procedures to describe metal fractionation in anaerobic granular sludges. *Talanta* **2005**, *65*, 549–558.

(20) Van der Veen, A.; Fermoso, F. G.; Lens, P. N. L. Bonding from analysis of metals and sulfur fractionation in methanol-grown anaerobic granular sludge. *Eng. Life Sci.* **2007**, *7*, 480–489.

(21) van Hullebusch, E. D.; Farges, F.; Lenz, M.; Lens, P. N. L.; Brown, G. E. J. Selenium speciation in biofilms from granular sludge bed reactors used for wastewater treatment. *AIP Conf. Proc. 882* **2007**, 229–231.

(22) Lenz, M.; Gmerek, A.; Lens, P. N.L. Selenium speciation in anaerobic granular sludge. *Int. J. Environ. Anal. Chem* **2006**, *86*, 615–627.

(23) Parodi, G.; Farges, F.; Gros, M.; Guiraud, M.; Miska, S. A Gandolfi chamber adapted to a curved multichannel detector for identifying mineral species. *Am. Mineral.* **2008**, submitted.

(24) Winterer, M. XAFS - A data analysis program for materials science. *J. Phys. IV* **1997**, *7*, C2.243C242.244.

(25) Farges, F.; Brown, G. E.; Petit, P.-E.; Munoz, M. Transition elements in water-bearing silicate glasses/melts. part I. a high-resolution and anharmonic analysis of Ni coordination environments in crystals, glasses, and melts. *Geochim. Cosmochim. Acta* **2001**, *65*, 1665–1678.

(26) Klementiev, K. V. *XANES Dactyloscope - Freeware for Windows*; available at http://www.desy.de/∼klmn/xanda.html (2006).

(27) Jalilehvand, F. Sulfur: not a silent element any more. *Chem. Soc. Rev.* **2006**, *35*, 1256–1268.

(28) Pickering, I. J.; Brown, G. E.; Tokunaga, T. K. Quantitative speciation of selenium in soils using X-ray-absorption spectroscopy. *Environ. Sci. Technol.* **1995**, *29*, 2456–2459.

(29) Sarret, G.; Avoscan, L.; Carriere, M.; Collins, R.; Geoffroy, N.; Carrot, F.; Coves, J.; Gouget, B. Chemical forms of selenium in the metal-resistant bacterium Ralstonia metallidurans CH34 exposed to selenite and selenate. *Appl. Environ. Microbiol.* **2005**, *71*, 2331–2337.

(30) Ryser, A. L.; Strawn, D. G.; Marcus, M. A.; Fakra, S.; Johnson-Maynard, J. L.; Moller, G. Microscopically focused synchrotron X-ray investigation of selenium speciation in soils developing on reclaimed mine lands. *Environ. Sci. Technol.* **2006**, *40*, 462–467.

(31) Kenward, P. A.; Fowle, D. A.; Yee, N. Microbial selenate sorption and reduction in nutrient limited systems. *Environ. Sci. Technol.* **2006**, *40*, 3782–3786.

(32) Manceau, A.; Gallup, D. L. Removal of selenocyanate in water by precipitation: characterization of copper-selenium precipitate by X-ray diffraction, infrared, and X-ray absorption spectroscopy. *Environ. Sci. Technol.* **1997**, *31*, 968–976.

(33) Buchanan, B. B.; Bucher, J. J.; Carlson, D. E.; Edelstein, N. M.; Hudson, E. A.; Kaltsoyannis, N.; Leighton, T.; Lukens, W.; Shuh, D. K.; Nitsche, H.; Reich, T.; Roberts, K.; Torretto, P.; Woicik, J.; Yang, W. S.; Yee, A.; Yee, B. C. A XANES and EXAFS investigation of the speciation of selenite following bacterial metabolization. *Inorg. Chem.* **1995**, *34*, 1617–1619.

(34) Shuh, D. K.; Kaltsoyannis, N.; Bucher, J. J.; Edelstein, N. M.; Clark, S. B.; Nitsche, H.; Almahamid,I.; Torretto, P.; Lukens, W.; Roberts, K.; Yee, B. C.; Carlson, D. E.; Yee, A.; Buchanan, B. B.; Leighton, T. In *Materials Research Society Symposium Proceedings*, San Francisco, April 5−7, 1994; Materials Research Society: Warrendale, PA,1994; Vol. *344*, pp 323−328.

(35) Ryser, A. L.; Strawn, D. G.; Marcus, M. A.; Johnson-Maynard, J. L.; Gunter, M. E.; Möller, G. Micro-spectroscopic investigation of selenium-bearing minerals from the Western US phosphate resource area. *Geochem. Trans.* **2005**, *6*, 1–11.

(36) Scheinost, A. C.; Charlet, L. Selenite reduction by mackinawite, magnetite and siderite: XAS characterization of nanosized redox products. *Environ. Sci. Technol.* **2008**, *42*, 1984–1989.

(37) Astratinei, V.; van Hullebusch, E. D.; Lens, P. N. L. Bioconversion of selenate in methanogenic anaerobic granular sludge. *J. Environ. Qual.* **2006**, *35*, 1873–1883.

(38) Azaroff, L. V.; Kaplow, R.; Kato, N. *X-Ray Diffraction*; McGraw-Hill: New York, 1974.
(39) Herbel, M. J.; Blum, J. S.; Oremland, R. S.; Borglin, S. E. Reduction of elemental selenium to selenide: experiments with anoxic sediments and bacteria that respire Se-oxyanions. *Geomicrobiol. J.* **2003**, *20*, 587–602.
(40) Chasteen, T. G.; Bentley, R. Biomethylation of selenium and tellurium: microorganisms and plants. *Chem. Rev.* **2003**, *103*, 1–25.
(41) Hockin, S.; Gadd, G. M. Removal of selenate from sulfate-containing media by sulfate-reducing bacterial biofilms. *Environ. Microbiol.* **2006**, *8*, 816–826.
(42) Hammel, C.; Kyriakopoulos, A.; Rösick, U.; Behne, D. Identification of selenocysteine and selenomethionine in protein hydrolysates by high-performance liquid chromatography of their o-phthaldialdehyde derivatives. *Analyst* **1997**, *122*, 1359–1363.
(43) Cutter, G. A.; Bruland, K. W. The marine biogeochemistry of selenium: a re-evaluation. *Limnol. Oceanogr.* **1984**, *29*, 1179–1192.
(44) Fisher, W. W.; Flores, F. A.; Henderson, J. A. Comparison of chalcocite dissolution in the oxygenated, aqueous sulfate and chloride systems. *Miner. Eng.* **1992**, *5*, 817–834.
(45) Seby, F.; Potin-Gautier, M.; Giffaut, E.; Borge, G.; Donard, O. F. X. A critical review of thermodynamic data for selenium species at 25°C. *Chem. Geol.* **2001**, *171*, 173–194.
(46) Peltier, E.; Dahl, A. L.; Gaillard, J. F. Metal speciation in anoxic sediments: when sulfides can be construed as oxides. *Environ. Sci. Technol.* **2005**, *39*, 311–316.
(47) Rickard, D.; Morse, J. W. Acid volatile sulfide (AVS). *Mar. Chem.* **2005**, *97*, 141–197.

ES800811Q